at room temperature (Ravi & Jagannathan, 1980). The antiferromagnetic structure obtained at room temperature is characterized by an A_z-type configuration. This configuration can be explained by the negative exchange interactions, J_1 and J_2 (see Fig. 3), between the Fe atoms situated in two corner-sharing tetrahedra. The periodicity of the magnetic unit cell, *i.e.* the propagation vector **k**, is determined by J_3 which is a superexchange interaction. This interaction is also negative as $\mathbf{k} = [0]$.

The results of neutron diffraction are in agreement with those of the Mössbauer effect. Both methods show that the magnetic moments of the Fe^{3+} ions are directed along the c axis of the unit cell, with a Néel temperature of about 690 K. This temperature is considerably lower than the 760 K obtained by Herrmann & Bacmann (1975). Cadée (1975) reported that his magnetic measurements carried out with a Faraday balance showed a Néel temperature higher than 1000 K. This unusually high value is inconsistent with our measurement of the disappearance of the magnetic contribution by neutron diffraction.

At room temperature the magnetic moment for the Fe^{3+} ion, 4·25 BM, is reduced by about 10% from the expected value for free Fe^{3+} (5 BM). This difference is probably due to the strong covalent character of the Fe^{3+}—O bond; but it seems that measurements of the electronic conductivity may confirm this.

The compound $BaSrFe_4O_8$ is isostructural with $BaCaFe_4O_8$ (Herrmann & Bacmann, 1971). The magnetic structures of the two compounds are very similar (Abbas, Mostafa & Fayek, 1982). From a structural point of view the substitution of strontium by calcium with smaller ionic radius may be expected to result in a decrease in the c value leaving the a value unchanged. The distance between the Fe^{3+} ions decreases, and this means that the magnetic interactions are stronger in the case of the Ca compound. Detailed data on the magnetic structure of $BaCaFe_4O_8$ are given elsewhere (Abbas *et al.*, 1982).

References

ABBAS, Y., MOSTAFA, F. & FAYEK, M. (1982). *J. Phys. Chem. Solids*. To be published.

BACON, G. E. (1972). *Acta Cryst.* A**28**, 357–358.

BATTI, P. (1962). *Ann. Chim.* (*Rome*), **52**, 1227.

BERTAUT, E. F. (1963). *Magnetism: Treatise on Modern Theory and Materials*, edited by G. T. RADO & H. SUHL, Vol. III, p. 150. New York: Academic Press.

BERTAUT, E. F. (1968). *Acta Cryst.* A**24**, 217–231.

BROCKHOUSE, B. N., CORLISS, L. M. & HASTING, J. M. (1955). *Phys. Rev.* **98**, 1721–1727.

CADÉE, M. C. (1975). *Acta Cryst.* B**31**, 2012–2015.

HERRMANN, D. & BACMANN, M. (1971). *Mater. Res. Bull.* **6**, 725–736.

HERRMANN, D. & BACMANN, M. (1975). *Acta Cryst.* B**31**, 665–668.

KANAMARU, F. & KIRIYAMA, R. (1964). *Mem. Inst. Sci. Ind. Res. Osaka Univ.* **21**, 89–110.

LANDAU, L. D. & LIFSHITZ, E. M. (1969). *Statistical Physics*, 2nd ed. Oxford: Pergamon Press.

LUCCHINI, E., MINICHELLI, D. & MERIANI, S. (1973). *Acta Cryst.* B**29**, 919–920.

MERIANI, S. & SLOCCARI, G. (1970). *Acta Cryst.* B**26**, 1184–1185.

RAVI, N. & JAGANNATHAN, R. (1980). *J. Phys. Chem. Solids*, **41**, 501–506.

Acta Cryst. (1983). B**39**, 4–10

On the Topotactic Dehydration $Ca_3(AsO_4)_2.11H_2O$ (Phaunouxite) → $Ca_3(AsO_4)_2.10H_2O$ (Rauenthalite), and the Structures of Both Minerals

BY MICHELE CATTI* AND GABRIELLA IVALDI

Istituto di Mineralogia, Cristallografia e Geochimica 'G. Spezia', Università di Torino, Via S. Massimo 22,
10123 *Torino, Italy*

(*Received* 3 *February* 1982; *accepted* 22 *April* 1982)

Abstract

Single crystals of the new mineral phaunouxite, $Ca_3(AsO_4)_2.11H_2O$ [a = 12·563 (7), b = 12·181 (6), c = 6·205 (4) Å, α = 88·94 (3), β = 91·67 (3), γ = 113·44 (4)°, V = 870·77 Å^3, M_r = 596·241, D_c = 2·274, D_m = 2·28 Mg m^{-3}, $F(000)$ = 600, μ(Mo $K\alpha$) = 4·8 mm^{-1}], form oriented intergrowths with rauenthalite, $Ca_3(AsO_4)_2.10H_2O$ [a = 12·564 (8), b = 12·169 (7), c = 6·195 (4) Å, α = 89·09 (3), β = 79·69 (3), γ = 118·58 (4)°, V = 812·65 Å^3, M_r = 578·226, D_c = 2·362, D_m = 2·36 Mg m^{-3}, $F(000)$ = 580, μ(Mo $K\alpha$) = 5·1 mm^{-1}], and dehydrate completely to that phase in dry air. The crystal structures of both minerals (space group $P\bar{1}$, Z = 2) were solved and least-squares-refined to R = 0·054 and 0·062, using 2715 and 1003 observed counter reflexions, respectively (Mo $K\alpha$ radiation). Isostructural (100) layers of

---

* Present address: Cattedra di Cristallochimica, Università di Milano, Via Golgi 19, 20133 Milano, Italy.

0567-7408/83/010004-07$01.50

Ca and As coordination polyhedra are present in both phases, and sandwich three (phaunouxite) or two (rauenthalite) independent water molecules (not Ca-coordinated) which provide the interlayer hydrogen bonds necessary for structure stability. Layers are shifted and spaced differently in the two structures. The topotactic dehydration of phaunouxite occurs by the loss of one lattice water molecule per asymmetric unit, followed by a rigid sliding and approaching of layers. The detailed mechanism of rearrangement of the interlayer hydrogen-bonding system is analyzed. Two other cases of topotactic dehydration reactions with a similar mechanism are compared and discussed.

Introduction

Rauenthalite and phaunouxite (Bari, Catti, Ferraris, Ivaldi & Permingeat, 1982) are secondary minerals produced by oxidation of arsenic ores in mines. Rauenthalite was synthetized by Guérin (1941). Both phases belong to the group of hydrated calcium arsenates $Ca_3(AsO_4)_2.nH_2O$, which includes the synthetic phases with $n = 0, 2, 3, 4, 5$ and 8 (Stahl-Brasse, Ariguib-Kbir & Guérin, 1971; Guérin, 1941; Pierrot, 1964). The mineral machatschkiite might be another member of this family, according to the formula $Ca_3(AsO_4)_2.9H_2O$ proposed by Walenta (1977); however, evidence of the presence of additional P or S was reported by Zemann, Effenberger & Mereiter (1981).

A close crystallographic association is observed between phaunouxite and rauenthalite (Bari *et al.*, 1982): all samples of the former mineral actually contain small amounts of the latter forming an oriented intergrowth; X-ray single-crystal photographs show the presence of both phases in apparently single crystals. Synthetic (but not natural) crystals of rauenthalite contain a similar kind of intergrowth. Moreover, crystals of phaunouxite dehydrate slowly to rauenthalite in dry air.

A structural study of both minerals was undertaken, following a line of research on the mechanisms of solid-state reactions in crystal hydrates; *cf.* previous work on the reactions $Ca_5H_2(AsO_4)_4.9H_2O$ (ferrarisite) → $Ca_5H_2(AsO_4)_4.5H_2O$ (dimorph of vladimirite) (Catti & Ivaldi, 1981), and $NaH_2PO_4.2H_2O \rightarrow NaH_2PO_4.H_2O$ (Catti & Ferraris, 1976).

Experimental and crystal data

Very small, acicular crystals of phaunouxite and rauenthalite from Sainte-Marie-aux-Mines (Alsace), elongated along [001], were kindly supplied by H. Bari (University of Strasbourg). A preliminary study by rotation and Weissenberg photography (Cu $K\alpha$ radiation) proved the symmetry to be triclinic and yielded approximate unit-cell constants for both minerals. The cell constant parallel to crystal elongation of rauenthalite (6·18 Å) has been reported in the literature (Pierrot, 1964). All crystals of phaunouxite examined showed some weak and diffuse spots due to rauenthalite on zero-layer Weissenberg photographs; the two lattices were related by a rotation of about 3° around the [001] elongation direction, with a superposition of their respective *hhl* rows. The sample of phaunouxite proved to be slightly dehydrated and consisted of an oriented intergrowth of the two minerals, showing that the dehydration reaction has a topotactic character. On the other hand, no traces of phaunouxite were detected on Weissenberg photographs of rauenthalite, and yet the latter mineral showed crystals of a much poorer quality and lower diffracting power than the former.

Two single crystals of phaunouxite and rauenthalite, with dimensions $0{\cdot}03 \times 0{\cdot}08 \times 0{\cdot}33$ and $0{\cdot}02 \times 0{\cdot}03 \times 0{\cdot}40$ mm respectively, were selected and used for measurements of unit-cell constants and diffraction intensities on a Philips PW 1100 four-circle automatic diffractometer (Mo $K\alpha$ radiation with graphite monochromator). The cell parameters determined by refinement of 25 measured θ values and crystal data are reported in the *Abstract*. The measurement conditions for data collection were the following: $\theta_{\rm max} = 27$ and 20°; scan mode $\omega/2\theta$ and ω; $\Delta\omega = 1{\cdot}8$ and 5°; scan speed 0·10 and 0·05° s^{-1}, respectively; the background time on each side of the peak was (scan time/2)$(I_{\rm bkg}/I_{\rm pk})^{1/2}$ for phaunouxite and 20 s for rauenthalite. An attenuating filter was inserted for peak intensities higher than 40 000 counts s^{-1}, and three reference reflexions were periodically checked. An experimental absorption correction based on the ψ scan of high-χ reflexions (North, Phillips & Mathews, 1968) was applied. All intensities with $I < 2\sigma(I)$ were considered unobserved and removed, giving two final sets of 2715 and 1003 reflexions, respectively, for phaunouxite and rauenthalite.

Determination of the structures

The program *MULTAN* based on direct methods (Germain, Main & Woolfson, 1971) was used to solve the two structures, which proved to be centrosymmetric from intensity statistics. In both cases, the solution with the highest combined figure of merit showed two As and three Ca atoms in general positions; all O atoms were revealed by subsequent structure-factor calculations and Fourier difference maps. Isotropic least-squares refinements converged to $R = 0{\cdot}067$ and $0{\cdot}078$ for phaunouxite and rauenthalite, respectively. Then anisotropic thermal factors were introduced for all atoms in the first case, and for

Table 1. *Atomic fractional coordinates and isotropic temperature factors* ($\times 10^2$ Å^2), *with e.s.d.'s in parentheses*

For phaunouxite and As and Ca atoms of rauenthalite $U_{eq} = \frac{1}{3}\sum_i \sum_j U_{ij} a_i^* a_j^* \mathbf{a}_i . \mathbf{a}_j$.

	Phaunouxite				Rauenthalite			
	x	y	z	U_{eq}	x	y	z	U_{eq} or U
As(1)	0·2598 (1)	0·1854 (1)	0·1645 (1)	0·97 (4)	0·2783 (2)	0·2190 (2)	0·0538 (4)	1·8 (2)
As(2)	0·0859 (1)	0·6283 (1)	0·7746 (1)	0·84 (4)	0·0903 (2)	0·6369 (2)	0·7388 (4)	1·6 (2)
Ca(1)	0·1682 (1)	0·5660 (1)	0·3208 (3)	1·08 (7)	0·1852 (4)	0·5871 (4)	0·2560 (8)	2·0 (3)
Ca(2)	0·1084 (1)	0·3372 (1)	0·8407 (3)	1·08 (7)	0·1258 (4)	0·3560 (4)	0·7921 (8)	1·8 (3)
Ca(3)	0·1605 (2)	0·9097 (2)	0·4957 (3)	1·20 (8)	0·1642 (4)	0·9274 (4)	0·4295 (8)	1·8 (3)
O(1)	0·1814 (6)	0·2015 (6)	−0·0493 (9)	1·8 (3)	0·195 (1)	0·223 (1)	−0·128 (2)	2·1 (4)
O(2)	0·1683 (6)	0·0845 (6)	0·3344 (10)	1·8 (3)	0·179 (1)	0·108 (1)	0·261 (2)	2·1 (4)
O(3)	0·3226 (6)	0·3166 (6)	0·2967 (10)	1·9 (3)	0·351 (1)	0·361 (1)	0·148 (2)	1·8 (4)
O(4)	0·3633 (5)	0·1436 (6)	0·0768 (10)	1·8 (3)	0·381 (1)	0·176 (1)	−0·073 (2)	2·2 (4)
O(5)	−0·0452 (5)	0·6345 (5)	0·8097 (9)	1·2 (3)	−0·052 (1)	0·621 (1)	0·832 (2)	1·4 (4)
O(6)	0·0535 (5)	0·4850 (5)	0·7066 (9)	1·3 (3)	0·064 (1)	0·494 (1)	0·674 (2)	2·2 (4)
O(7)	0·1501 (5)	0·7135 (5)	0·5617 (9)	1·2 (3)	0·158 (1)	0·732 (1)	0·506 (2)	2·3 (4)
O(8)	0·1687 (5)	0·6715 (5)	0·9993 (9)	1·4 (3)	0·176 (1)	0·688 (1)	0·929 (2)	1·6 (4)
W(1)	0·3618 (6)	0·7127 (7)	0·3905 (12)	2·9 (4)	0·387 (1)	0·765 (1)	0·224 (3)	3·1 (4)
W(2)	0·2515 (6)	0·4467 (6)	0·5563 (10)	1·9 (3)	0·289 (1)	0·484 (1)	0·453 (2)	1·9 (4)
W(3)	0·2759 (5)	0·4839 (6)	0·0635 (10)	1·6 (3)	0·307 (1)	0·523 (1)	−0·057 (3)	2·9 (4)
W(4)	0·0554 (5)	0·2158 (5)	0·5053 (9)	1·4 (3)	0·067 (1)	0·227 (1)	0·482 (2)	2·0 (4)
W(5)	−0·0879 (6)	0·1696 (6)	0·8650 (9)	1·8 (3)	−0·093 (1)	0·160 (1)	0·904 (2)	1·9 (4)
W(6)	0·0719 (6)	0·9804 (5)	0·7864 (10)	1·8 (3)	0·071 (1)	0·984 (1)	0·760 (2)	1·4 (4)
W(7)	0·3377 (7)	0·9390 (8)	0·3182 (13)	4·0 (5)	0·364 (1)	0·986 (1)	0·179 (2)	2·4 (4)
W(8)	0·3003 (8)	0·9697 (8)	0·7735 (12)	4·8 (5)	0·315 (2)	1·007 (2)	0·647 (3)	4·0 (5)
W(9)	0·4023 (7)	0·8017 (8)	0·8229 (14)	3·9 (5)	0·414 (2)	0·850 (2)	0·681 (3)	3·5 (5)
W(10)	0·4349 (7)	0·3049 (7)	0·7068 (13)	3·2 (4)	0·486 (2)	0·342 (2)	0·445 (3)	4·4 (5)
W(11)	0·4536 (6)	0·5426 (7)	0·7790 (12)	2·7 (4)				

As and Ca atoms only in the second, and full-matrix refinements (unit weights) led to $R = 0{\cdot}057$ and 0·062, respectively. At this stage the analysis was continued for phaunouxite only: 15 H atoms out of 22 were located on a difference map and included in the refinement; however, since better interatomic distances and angles were obtained from unrefined positions, the final cycle was performed with fixed parameters for H atoms (temperature factors $U = 0{\cdot}03$ Å^2), and $R = 0{\cdot}054$ was reached. Atomic fractional coordinates and equivalent isotropic or isotropic thermal parameters are reported (except for H atoms) in Table 1; coordinates of phaunouxite H atoms appear in Table 2.* The same atomic symbols are used for both asymmetric units, to stress the close correspondence of structural features which is discussed below. Results of the structure determination are less satisfactory for rauenthalite than for phaunouxite, mainly because of the higher e.s.d.'s, due to the use of fewer data. All calculations were performed by the *SHELX* package of crystallographic programs (Sheldrick, 1976) and the scattering factors for neutral atoms are those reported in *International Tables for X-ray Crystallography* (1974).

Discussion

Common intralayer structural features

The crystal structures of phaunouxite and rauenthalite are built up by (100) layers of AsO_4 distorted tetrahedra and Ca coordination polyhedra sharing vertices and edges, which are shifted in the two cases and sandwich three or two 'lattice' (*i.e.* not Ca-coordinated) water molecules, respectively; hydrogen bonds provide the necessary interlayer linking. This layered structure accounts well for the perfect {100} cleavage observed in both minerals (Pierrot, 1964; Bari *et al.*, 1982). The layers of coordination polyhedra are substantially isostructural in the two phases, as is shown in Figs. 1 and 2 and in Tables 3 and 4, reporting bond distances of Ca polyhedra and distances and angles of As tetrahedra, respectively.

The three independent Ca atoms have coordination numbers of 8, 7, 7, and their polyhedra are characterized by an increase of the number of coordinated water molecules and by a decrease of the shared geometrical elements in the sequence Ca(1) → Ca(2) → Ca(3).* Four edges are shared by the Ca(1) poly-

---

* Lists of structure factors and anisotropic temperature factors for both minerals and Table 2 have been deposited with the British Library Lending Division as Supplementary Publication No. SUP 36938 (26 pp.). Copies may be obtained through The Executive Secretary, International Union of Crystallography, 5 Abbey Square, Chester CH1 2HU, England.

* An unprimed figure in parentheses denotes an atom of the asymmetric unit; primed figures mean atoms subjected to the transformation $\bar{x},\bar{y},\bar{z}$; roman numerals represent the translations: (I) +**b** + **c**; (II) +**b** + 2**c**; (III) +**a** + **b** + **c**; (IV) −**c**; (V) +**c**; (VI) +**b**; (VII) +**a** + **b**; (VIII) +**a** + 2**b** + **c**.

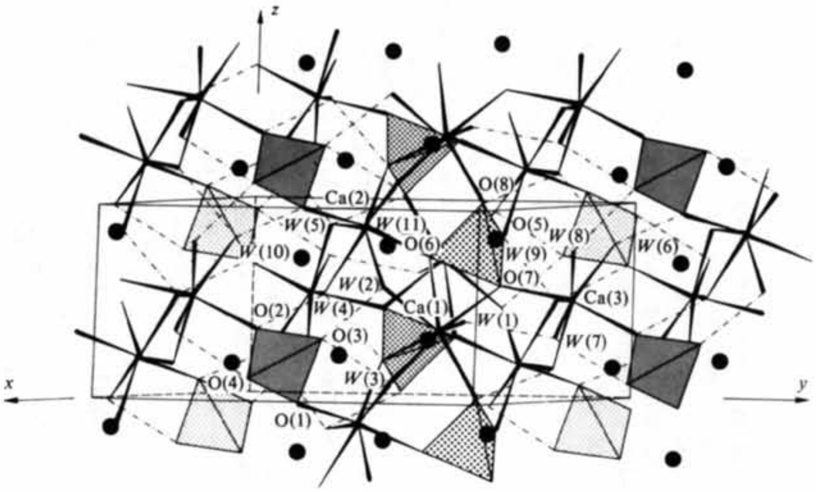

Fig. 1. Orthogonal projection of a single (100) layer of the structure of phaunouxite, $Ca_3(AsO_4)_2.11H_2O$. AsO_4 tetrahedra, Ca–O coordination bonds (black rods) and intralayer hydrogen bonds (dashed–dotted lines) are emphasized. Black circles represent interlayer water molecules.

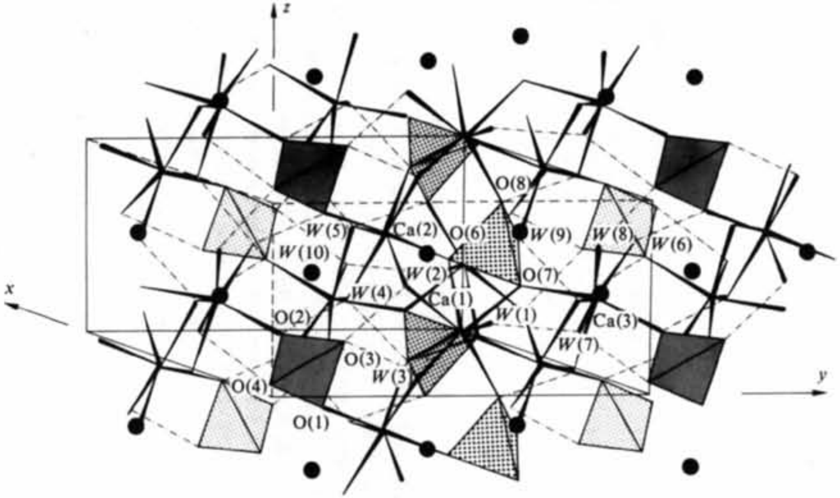

Fig. 2. Orthogonal projection of a single (100) layer of the structure of rauenthalite, $Ca_3(AsO_4)_2.10H_2O$. Substantial isostructurality with phaunouxite, except for interlayer water molecules, is apparent.

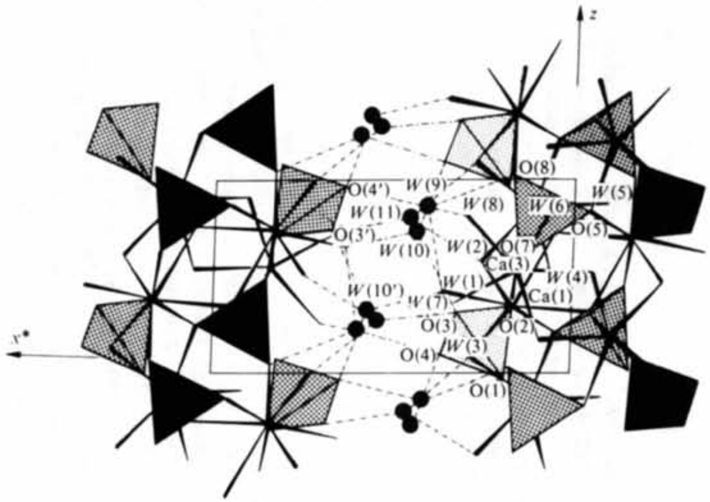

Fig. 3. Projection of the crystal structure of phaunouxite, $Ca_3(AsO_4)_2.11H_2O$, onto the plane containing the **c** and **a*** directions. Interlayer water molecules (black circles) and hydrogen bonds (dashed–dotted lines) are emphasized.

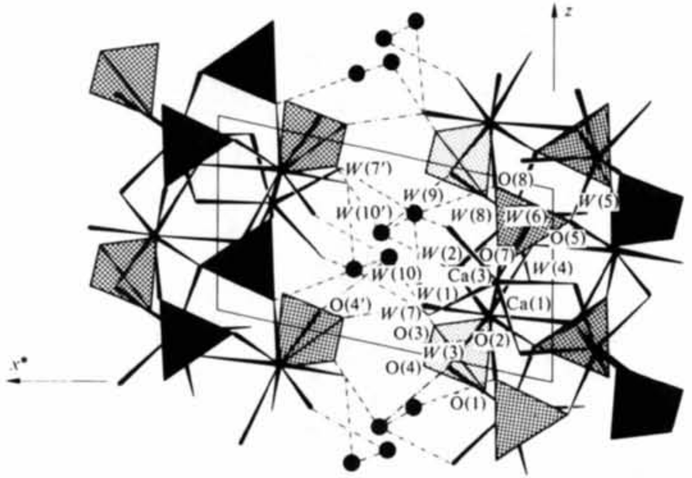

Fig. 4. Projection of the crystal structure of rauenthalite, $Ca_3(AsO_4)_2.10H_2O$, onto the plane containing the **c** and **a*** directions. Adjacent layers are shifted with respect to the phaunouxite structure, as a consequence of dehydration.

Table 3. *Interatomic distances* (Å) *in the* Ca *coordination polyhedra of phaunouxite* (*ph.*) *and rauenthalite* (*r.*), *with e.s.d.'s in parentheses*

	ph.	r.		ph.	r.		ph.	r.
Ca(1)–O(6)	2·786 (6)	2·67 (1)	Ca(2)–O(1)$^{\mathrm{V}}$	2·273 (7)	2·26 (1)	Ca(3)–O(2)$^{\mathrm{VI}}$	2·303 (7)	2·33 (1)
Ca(1)–O(7)	2·441 (6)	2·47 (1)	Ca(2)–O(6)	2·304 (6)	2·32 (1)	Ca(3)–O(7)	2·370 (7)	2·38 (1)
Ca(1)–O(8)$^{\mathrm{IV}}$	2·352 (6)	2·40 (1)	Ca(2)–O(5′)$^{\mathrm{II}}$	2·409 (6)	2·42 (1)	Ca(3)–W(4′)$^{\mathrm{I}}$	2·529 (7)	2·54 (1)
Ca(1)–O(5′)$^{\mathrm{I}}$	2·451 (6)	2·41 (1)	Ca(2)–W(2)	2·513 (7)	2·52 (1)	Ca(3)–W(5′)$^{\mathrm{I}}$	2·456 (6)	2·45 (1)
Ca(1)–O(6′)$^{\mathrm{I}}$	2·602 (6)	2·74 (1)	Ca(2)–W(3)$^{\mathrm{V}}$	2·542 (7)	2·57 (1)	Ca(3)–W(6)	2·484 (7)	2·45 (1)
Ca(1)–W(1)	2·409 (8)	2·39 (1)	Ca(2)–W(4)	2·492 (6)	2·49 (1)	Ca(3)–W(7)	2·407 (9)	2·47 (1)
Ca(1)–W(2)	2·527 (7)	2·62 (1)	Ca(2)–W(5)	2·505 (8)	2·59 (1)	Ca(3)–W(8)	2·332 (9)	2·35 (2)
Ca(1)–W(3)	2·577 (7)	2·62 (2)	Average	2·434	2·45	Average	2·412	2·42
Average	2·518	2·54						

Table 4. *Interatomic distances* (Å) *and* O–As–O *angles* (°) *in the* AsO_4 *groups of phaunouxite* (*ph.*) *and rauenthalite* (*r.*), *with e.s.d.'s in parentheses*

	ph.	r.		ph.	r.
As(1)–O(1)	1·684 (6)	1·68 (1)	As(2)–O(5)	1·699 (9)	1·69 (1)
As(1)–O(2)	1·686 (7)	1·67 (1)	As(2)–O(6)	1·686 (6)	1·68 (1)
As(1)–O(3)	1·690 (7)	1·70 (1)	As(2)–O(7)	1·679 (6)	1·65 (1)
As(1)–O(4)	1·681 (6)	1·69 (1)	As(2)–O(8)	1·676 (6)	1·66 (1)
Average	1·685	1·69	Average	1·685	1·67

	ph.	r.	ph.	r.
O(1)–O(2)	2·727 (9)	2·69 (2)	108·1 (3)	106·9 (6)
O(1)–O(3)	2·763 (9)	2·78 (2)	109·9 (3)	110·7 (6)
O(1)–O(4)	2·737 (10)	2·73 (2)	108·9 (3)	108·2 (6)
O(2)–O(3)	2·729 (10)	2·77 (2)	107·9 (3)	110·7 (6)
O(2)–O(4)	2·803 (9)	2·73 (2)	112·8 (4)	108·9 (6)
O(3)–O(4)	2·751 (10)	2·79 (2)	109·4 (4)	111·4 (6)
Average	2·752	2·75	109·5	109·5

	ph.	r.	ph.	r.
O(5)–O(6)	2·674 (9)	2·68 (2)	104·4 (3)	105·2 (6)
O(5)–O(7)	2·757 (9)	2·73 (2)	109·4 (3)	109·8 (6)
O(5)–O(8)	2·771 (9)	2·76 (2)	110·4 (3)	110·7 (6)
O(6)–O(7)	2·704 (9)	2·66 (2)	107·0 (3)	106·1 (6)
O(6)–O(8)	2·817 (8)	2·79 (2)	113·9 (3)	113·2 (6)
O(7)–O(8)	2·774 (8)	2·74 (2)	111·6 (3)	111·5 (6)
Average	2·750	2·73	109·4	109·4

hedron with two As(2)-type and two Ca(2)-type polyhedra, while Ca(2) shares three edges and Ca(3) only one edge with other neighboring Ca polyhedra. A similar difference is observed between the As(1) and As(2) tetrahedra: the latter shares two edges [O(5)–O(6) and O(6)–O(7)] and all vertices with Ca polyhedra, whereas the former shares just two vertices O(1) and O(2).

Thus, the degree of condensation of coordination polyhedra is not homogeneous throughout a whole single layer, but changes periodically along the [010] direction and is constant along [001]. Then the internal structure of layers is made up by [001] strips repeated by the **b** vector, each of which contains a central chain of highly condensed Ca(1), Ca(2) and As(2) polyhedra, with the Ca(3) and As(1) polyhedra attached on its sides and involved in most intralayer hydrogen bonds (Tables 5 and 6). Adjacent strips are loosely bonded by the only Ca(3)–O(2)$^{\mathrm{VI}}$ coordination bond and by the hydrogen bonds W(6)···O(1)$^{\mathrm{I}}$ and W(8)···O(4)$^{\mathrm{I}}$ (and their equivalent ones by symmetry). This structural scheme explains the good {010} cleavage observed by Bari *et al.* (1982).

Lattice water molecules and hydrogen bonding

In hydrated oxysalts, Ca^{2+} cations show a lower affinity for water molecules than do other cations with higher charge density (*e.g.* Mg^{2+}), so that fully hydrated Ca coordination polyhedra have never been observed. On the other hand, Ca polyhedra usually have a strong tendency to condense with one another by sharing several edges and vertices. For these reasons, Ca crystal hydrates with a high content of water very often crystallize in layered structures with a significant fraction of water molecules not Ca-coordinated and located between layers; *cf.* the cases of picropharmacolite, $Ca_4MgH_2(AsO_4)_4.11H_2O$ (Catti, Ferraris & Ivaldi, 1981), and ferrarisite, $Ca_5H_2(AsO_4)_4.9H_2O$ (Catti, Chiari & Ferraris, 1980). A similar situation is observed for phaunouxite and rauenthalite, where three [W(9), W(10), W(11)] out of eleven and two [W(9), W(10)] out of ten water molecules, respectively, are involved in interlayer hydrogen bonding only (Figs. 3 and 4).

These lattice water molecules are arranged along [010] chains, and each generally forms four O···O contacts with a roughly tetrahedral disposition. The assignment of the donor and acceptor hydrogen-bonding functions is unambiguous in phaunouxite (Table 5), since most H atoms have been located. Unusually large acceptor···donor···acceptor angles are observed for the W(7) and W(9) water molecules (153 and 141°, respectively). In the case of rauenthalite, where H atoms could not be located, two alternative hydrogen-bonding schemes are possible for the three H_2O molecules W(1), W(7) and W(9), and are reported in separate columns of Table 6. Although the second configuration (right-hand column in Table 6) is similar to that observed for phaunouxite, it is less probable than the first because of the very large O(4)$^{\mathrm{VI}}$···W(7)···W(1) and O(8)···W(9)···W(7′)$^{\mathrm{VIII}}$ angles (150·5 and 130·2°, respectively). The two configurations are related by rotations of each of these molecules around a fixed W–H bond direction, so that the other W–H′ bond points toward two alternative acceptors: for instance, W(9) keeps the hydrogen bond W(9)···O(8) fixed, and donates another bond either to W(1) or to W(7′)$^{\mathrm{VIII}}$. In rauenthalite,

Table 5. *Interatomic distances* (Å) *and angles* (°) *for hydrogen bonds in phaunouxite, with e.s.d.'s in parentheses*

D H *A*	*D*–*A*	*D*–H	H–*A*	*DHA*	H*D*H′	*ADA*′
$W(1)\text{–H}(1)\cdots W(9)$	2·87 (1)	0·97	1·92	166		103·5 (3)
$W(1)\cdots\cdots W(10')^{\mathrm{III}}$	2·73 (1)					
$W(2)\text{–H}(2)\cdots\mathrm{O}(3)$	2·68 (1)	0·76	2·02	147	108	94·9 (3)
$W(2)\text{–H}(3)\cdots W(11)$	2·69 (1)	0·92	1·83	154		
$W(3)\text{–H}(4)\cdots\mathrm{O}(3)$	2·72 (1)	1·00	1·73	172	100	98·0 (3)
$W(3)\text{–H}(5)\cdots W(11)^{\mathrm{IV}}$	2·74 (1)	0·82	2·02	147		
$W(4)\text{–H}(6)\cdots\mathrm{O}(2)$	2·766 (9)	0·94	1·85	164	112	105·9 (3)
$W(4)\text{–H}(7)\cdots\mathrm{O}(5')^{\mathrm{I}}$	2·684 (8)	0·75	1·95	170		
$W(5)\text{–H}(8)\cdots\mathrm{O}(8')^{\mathrm{II}}$	2·676 (9)	1·02	1·70	159	106	110·7 (3)
$W(5)\text{–H}(9)\cdots W(6')^{\mathrm{II}}$	2·860 (9)	0·69	2·24	150		
$W(6)\text{–H}(10)\cdots\mathrm{O}(2')^{\mathrm{I}}$	2·88 (1)	0·88	2·07	154	113	115·3 (3)
$W(6)\text{–H}(11)\cdots\mathrm{O}(1)^{\mathrm{I}}$	2·694 (9)	0·83	1·87	170		
$W(7)\cdots\cdots\mathrm{O}(4)^{\mathrm{VI}}$	2·79 (1)					153·4 (4)
$W(7)\cdots\cdots W(1)$	2·92 (1)					
$W(8)\text{–H}(12)\cdots\mathrm{O}(4)^{\mathrm{I}}$	2·72 (1)	0·80	2·02	146	92	115·6 (4)
$W(8)\text{–H}(13)\cdots W(9)$	2·82 (1)	0·89	1·99	155		
$W(9)\cdots\cdots\mathrm{O}(8)$	2·96 (1)					140·9 (4)
$W(9)\cdots\cdots\mathrm{O}(4')^{\mathrm{III}}$	2·80 (1)					
$W(10)\cdots\cdots\mathrm{O}(3)$	2·90 (1)					133·1 (4)
$W(10)\cdots\cdots\mathrm{O}(4)^{\mathrm{V}}$	2·91 (1)					
$W(11)\text{–H}(14)\cdots\mathrm{O}(3')^{\mathrm{III}}$	2·70 (1)	0·83	1·88	165	91	104·9 (4)
$W(11)\text{–H}(15)\cdots W(10)$	2·85 (1)	0·95	1·93	163		

Table 6. *Interatomic distances* (Å) *and angles* (°) *of hydrogen bonds in rauenthalite, with e.s.d.'s in parentheses*

D *A*	*D*–*A*	*ADA*′	*D* *A*	*ADA*′
$W(1)\cdots\mathrm{O}(4')^{\mathrm{VII}}$	2·62 (2)	109·0 (6)	$W(1)\cdots\mathrm{O}(4')^{\mathrm{VII}}$	97·5 (7)
$W(1)\cdots W(7)$	2·85 (2)		$W(1)\cdots W(9)$	
$W(2)\cdots\mathrm{O}(3)$	2·66 (2)	104·6 (7)		
$W(2)\cdots W(10')^{\mathrm{III}}$	2·80 (3)			
$W(3)\cdots\mathrm{O}(3)$	2·65 (2)	107·6 (7)		
$W(3)\cdots W(10')^{\mathrm{VII}}$	2·96 (3)			
$W(4)\cdots\mathrm{O}(2)$	2·70 (2)	106·5 (5)		
$W(4)\cdots\mathrm{O}(5')^{\mathrm{I}}$	2·76 (2)			
$W(5)\cdots\mathrm{O}(8')^{\mathrm{II}}$	2·66 (2)	111·8 (6)		
$W(5)\cdots W(6')^{\mathrm{II}}$	2·83 (2)			
$W(6)\cdots\mathrm{O}(2')^{\mathrm{I}}$	2·81 (2)	116·9 (6)		
$W(6)\cdots\mathrm{O}(1)^{\mathrm{I}}$	2·74 (2)			
$W(7)\cdots\mathrm{O}(4)^{\mathrm{VI}}$	2·67 (2)	91·5 (6)	$W(7)\cdots\mathrm{O}(4)^{\mathrm{VI}}$	150·5 (7)
$W(7)\cdots W(9')^{\mathrm{VIII}}$	2·85 (3)		$W(7)\cdots W(1)$	
$W(8)\cdots\mathrm{O}(4)^{\mathrm{I}}$	2·63 (2)	111·2 (10)		
$W(8)\cdots W(9)$	2·76 (3)			
$W(9)\cdots\mathrm{O}(8)$	2·79 (3)	100·9 (8)	$W(9)\cdots\mathrm{O}(8)$	130·2 (8)
$W(9)\cdots W(1)$	3·05 (3)		$W(9)\cdots W(7')^{\mathrm{VIII}}$	
$W(10)\cdots\mathrm{O}(3)$	2·79 (2)	112·3 (8)		
$W(10)\cdots W(9')^{\mathrm{III}}$	3·19 (3)			

W(9) shows a fifth long contact (3·19 Å) with *W*(10′), so that the molecule would seem to donate two and receive three hydrogen bonds, showing an unusual configuration. In both structures all lattice water molecules are hydrogen-bonded to at least one O atom, and none has an ice-like environment (four $W\cdots W$ contacts) as is observed, for instance, in picropharmacolite (Catti *et al.*, 1981). The interlayer bonding is achieved *via* lattice water molecules only in phaunouxite, whereas in rauenthalite a 'direct' linkage is also provided by the $W(1)\cdots\mathrm{O}(4')^{\mathrm{VII}}$ hydrogen bond.

Mechanism of the topotactic dehydration

Phaunouxite and rauenthalite substantially share the same *a*, *b*, *c* and α lattice constants, and differ for the β and γ angles only (see *Abstract*). The (100) lattice planes, corresponding to isostructural layers of coordination polyhedra, have a common periodic pattern but are shifted and spaced differently in the two crystal structures, according to the different orientations of the **a** vectors which repeat them. The d_{100} interplanar spacing decreases from phaunouxite (11·53 Å) to rauenthalite (10·79 Å). Sliding of (100) planes, occurring in the transformation from the higher to the lower hydrate, can be expressed by the interlayer shift vector $\mathbf{s} = -0{\cdot}087\mathbf{b} + 0{\cdot}425\mathbf{c}$, which has its largest component along the [001] direction. In order to cancel the effect of different obliquities of the **a** vectors with respect to (100) planes, the atomic fractional coordinates of the two asymmetric units should be referred to ($\mathbf{a}^*$,**b**,**c**) frames, proving then to be nearly identical in accordance with the isostructurality of layers [larger shifts are observed for the *W*(9) and *W*(10) water molecules].

The following detailed mechanism can be proposed for the reaction $\mathrm{Ca_3(AsO_4)_2.11H_2O}$ (phaunouxite) → $\mathrm{Ca_3(AsO_4)_2.10H_2O}$ (rauenthalite) + $\mathrm{H_2O}$. When dehydration starts, the *W*(11) and *W*(11′) molecules break their hydrogen bonds and escape. A rearrangement of interlayer hydrogen bonding is then necessary, so that the (100) layers slide rigidly 2·82 Å along the **s** direction and approach by 0·74 Å, in order to face each other in a suitable position. The two remaining lattice water molecules, *W*(9) and *W*(10), have changed their positions very little with respect to the layer containing the asymmetric unit (right-hand layer in Fig. 3); however, the symmetry center has shifted so that now *W*(10′) occupies approximately the former position of *W*(11). Then the hydrogen bonds $W(2)\cdots W(11)$ and $W(3)\cdots W(11)^{\mathrm{IV}}$ are replaced by $W(2)\cdots W(10')^{\mathrm{III}}$ and $W(3)\cdots W(10')^{\mathrm{VII}}$, respectively; the other two hydrogen bonds involving *W*(11), *i.e.* $W(11)\cdots\mathrm{O}(3')^{\mathrm{III}}$ and $W(11)\cdots W(10)$, are suppressed. The slight shift of *W*(10) is sufficient to break the $W(10)\cdots\mathrm{O}(4)^{\mathrm{V}}$ bond and to substitute it by the long contact $W(10)\cdots W(9')^{\mathrm{III}}$. But the key role in rearranging the interlayer linking is played by the new bonds $W(9)\cdots W(7')^{\mathrm{VIII}}$ and $W(1)\cdots\mathrm{O}(4')^{\mathrm{VII}}$ of rauenthalite, which replace $W(9)\cdots\mathrm{O}(4')^{\mathrm{III}}$ and $W(1)\cdots W(10')^{\mathrm{III}}$ of phaunouxite, respectively. In particular, the strong hydrogen bond $W(1)\cdots\mathrm{O}(4')^{\mathrm{VII}}$ (2·63 Å) ties directly coordination polyhedra of adjacent layers, without involving any lattice water molecules, in the lower hydrate phase; thus the loss of *W*(11) is compensated somehow.

Comparison with other topotactic dehydration reactions

Solid-state topotactic reactions were divided by Günter & Oswald (1977) into five types, according to their structural mechanism. The dehydration of phaunouxite into rauenthalite can be classified as a reaction of the type in which two-dimensional elements (layers) are conserved.

The activation energy for all these 'layer-conserving' dehydration processes is surely very small owing to the small number of bonds broken and reconstructed during the reactions. This should be particularly true for mechanisms involving loss of lattice H_2O molecules, where only low-energy hydrogen bonds are broken, as in the present case and in other examples, *e.g.* the dehydration of $MoO_3.2H_2O$ (Günter, 1972). On these grounds the oriented intergrowth of phaunouxite and rauenthalite observed in natural crystals at room temperature can be easily understood. A slightly different mechanism is observed for the dehydration of $Ca_5H_2(AsO_4)_4.9H_2O$ (Catti & Ivaldi, 1981), where interlayer H_2O—Ca bonds are also broken, in addition to hydrogen bonds, so that a higher activation energy should be necessary for that reaction.

We thank H. Bari (University of Strasbourg) for providing the samples of phaunouxite and rauenthalite used in this study, and Professor G. Ferraris (Università di Torino) for help with data collection and for stimulating discussions. The X-ray intensities were measured at the Centro di Studio del CNR per la Cristallografia Strutturale, Pavia. Research was supported financially by the Consiglio Nazionale delle Ricerche, Roma.

References

BARI, H., CATTI, M., FERRARIS, G., IVALDI, G. & PERMINGEAT, F. (1982). *Bull. Minéral.* In the press.
CATTI, M., CHIARI, G. & FERRARIS, G. (1980). *Bull Minéral.* **103**, 541–546.
CATTI, M. & FERRARIS, G. (1976). *Acta Cryst.* B**32**, 359–363.
CATTI, M., FERRARIS, G. & IVALDI, G. (1981). *Am. Mineral.* **66**, 385–391.
CATTI, M. & IVALDI, G. (1981). *Z. Kristallogr.* **157**, 119–130.
GERMAIN, G., MAIN, P. & WOOLFSON, M. M. (1971). *Acta Cryst.* A**27**, 368–376.
GUÉRIN, H. (1941). *Ann. Chim. (Paris)*, **16**, 101–153.
GÜNTER, J. R. (1972). *J. Solid State Chem.* **5**, 354–359.
GÜNTER, J. R. & OSWALD, H. R. (1977). *J. Solid State Chem.* **21**, 211–215.
International Tables for X-ray Crystallography (1974). Vol. IV. Birmingham: Kynoch Press.
NORTH, A. C. T., PHILLIPS, D. C. & MATHEWS, F. S. (1968). *Acta Cryst* A**24**, 351–359.
PIERROT, R. (1964). *Bull. Soc. Fr. Minéral. Cristallogr.* **87**, 169–211.
SHELDRICK, G. M. (1976). *SHELX* 76. Program for crystal structure determination. Univ. of Cambridge, England.
STAHL-BRASSE, R., ARIGUIB-KBIR, N. & GUÉRIN, H. (1971). *Bull. Soc. Chim. Fr.* pp. 2828–2832.
WALENTA, K. (1977). *Tschermaks Mineral. Petrogr. Mitt.* **24**, 125–132.
ZEMANN, J., EFFENBERGER, H. & MEREITER, K. (1981). *Anz. Österr. Akad. Wiss. Math. Naturwiss. Kl.* No. 2, pp. 15–17.

Acta Cryst. (1983). B**39**, 10–17

A Description of the Leucophoenicite Family of Structures and its Relation to the Humite Family

BY T. J. WHITE AND B. G. HYDE

Research School of Chemistry, Australian National University, PO Box 4, *Canberra, ACT* 2600, *Australia*

(*Received* 28 *August* 1981; *accepted* 12 *July* 1982)

Abstract

Two distinct though closely related structural families are described. One, which we call the leucophoenicite family, consists of mimetically twinned, cubic-close-packed (c.c.p.) arrays of A cations with B cations in A_6 trigonal prisms in the composition planes and anions in (usually) BA_3 tetrahedra. A general 'twin formula' may be written as $(1,2^x)$, the twin individuals being one and two cations wide. (The superscript x indicates the number of consecutive twin lamellae of thickness 2.) The other is the humite family which has twin individuals two or three cations wide and twin formula $(2^x,3)$. In addition to the type structures such as leucophoenicite and the humite minerals which are all silicates there are also borates, germanates, *etc.* whose cation arrays place them in these families, especially the former.

Introduction

It has frequently been noted that the structures of leucophoenicite and some related compounds and those of forsterite (olivine) and of the humite minerals (norbergite, chondrodite, humite and clinohumite) have common geometrical features. Moore (1970) determined the structure of leucophoenicite, and used a module of five edge-sharing MO_6 octahedra, 'the generalized olivine type', to construct a leucophoen-

0567-7408/83/010010-08$01.50